

## Zeeman Splitting in Ballistic Hole Quantum Wires

R. Danneau,<sup>1,\*</sup> O. Klochan,<sup>1</sup> W. R. Clarke,<sup>1</sup> L. H. Ho,<sup>1</sup> A. P. Micolich,<sup>1</sup> M. Y. Simmons,<sup>1</sup> A. R. Hamilton,<sup>1</sup> M. Pepper,<sup>2</sup>  
D. A. Ritchie,<sup>2</sup> and U. Zülicke<sup>3</sup>

<sup>1</sup>*School of Physics, University of New South Wales, Sydney 2052, Australia*

<sup>2</sup>*Cavendish Laboratory, Madingley Road, Cambridge CB3 0HE, United Kingdom*

<sup>3</sup>*Institute of Fundamental Sciences and MacDiarmid Institute for Advanced Materials and Nanotechnology, Massey University, Palmerston North, New Zealand*

(Received 12 December 2005; published 11 July 2006)

We have studied the Zeeman splitting in ballistic hole quantum wires formed in a (311)A quantum well by surface gate confinement. Transport measurements clearly show lifting of the spin degeneracy and crossings of the subbands when an in-plane magnetic field  $B$  is applied parallel to the wire. When  $B$  is oriented perpendicular to the wire, no spin splitting is discernible up to  $B = 8.8$  T. The observed large Zeeman splitting anisotropy in our hole quantum wires demonstrates the importance of quantum confinement for spin splitting in nanostructures with strong spin-orbit coupling.

DOI: [10.1103/PhysRevLett.97.026403](https://doi.org/10.1103/PhysRevLett.97.026403)

PACS numbers: 71.70.-d, 73.21.Hb, 73.23.Ad

Studying the spin degree of freedom of charge carriers in semiconductors has become an area of significant current interest, not only for fundamental understanding of spin, but also for potential applications that use spin, rather than charge, in electronic components [1]. Spin polarized currents can be created by applying magnetic fields, using magnetic leads or ferromagnetic semiconductors. Alternatively, the intrinsic coupling between spin state and orbital motion of quantum particles opens up intriguing possibilities for implementing a spin-electronics paradigm. For example, it has been proposed to tune the spin splitting by using an external electric field in systems exhibiting strong spin-orbit coupling [2]. In such devices, a spin-polarized current could be manipulated in a ballistic channel by only tuning a gate voltage [3]. As valence-band states are predominantly  $p$ -like (unlike conduction-band states which are  $s$ -like), spin-orbit effects are particularly important in confined hole systems based on GaAs [4]. This makes holes in GaAs especially interesting for studies of spin-controlled devices. In addition, the fact that holes near the valence-band edge are spin-3/2 particles leads to intriguing quantum effects such as the suppression of Zeeman splitting for in-plane field directions in typical two-dimensional (2D) hole systems [5]. How further confinement of holes moving in a narrow wire affects their peculiar spin properties has not been investigated in detail before, which motivates our present study. Furthermore, Zeeman splitting of one-dimensional (1D) subband bottoms can be *directly* measured using the phenomenon of conductance quantization [6–9].

We have performed an experimental study of the Zeeman splitting of quantum wires in the ballistic regime, formed by a lateral confinement of a 2D heavy-hole (HH) system that was grown on the (311)A surface of a GaAs/Al<sub>x</sub>Ga<sub>1-x</sub>As heterostructure. Previous works on 2D systems [4,10,11] identified an anisotropic effective Landé  $g$ -factor  $g^*$  for in-plane magnetic fields applied in

the  $[\bar{2}33]$  and  $[01\bar{1}]$  directions. In our 1D system, which is aligned with the  $[\bar{2}33]$  direction, when we apply an in-plane  $B$  we measure a much larger  $g^*$  anisotropy between parallel to the wire ( $B_{\parallel}$ ) and perpendicular to the wire ( $B_{\perp}$ ) than is predicted (and observed) for 2D HH systems [12]. We attribute these observations to the interplay between quantum confinement and strong spin-orbit coupling present in the valence band. Our results show that it is possible to engineer magnetic (Zeeman) splitting by tuning the electric confinement in hole nanostructures.

In our experiments, we used the same 1D hole bilayer system as described previously [13] and we have measured the differential conductance in the top wire of the bilayer [14]. Measurements were done in a dilution refrigerator with a base temperature of  $T = 20$  mK. Side gates and a middle gate used to form the quantum wire are aligned along the  $[\bar{2}33]$  direction. Electrical measurements have been performed using standard low-frequency ac lock-in techniques with an excitation voltage of  $20 \mu\text{V}$  at 17 Hz. We used two side gates to create the 1D channels and the back and middle gates to control the density and the confinement potential as described in [13].

Figure 1(a) shows the differential conductance,  $G = dI/dV$  as a function of side gate voltage  $V_{\text{SG}}$  for different in-plane magnetic fields parallel to the wire  $B_{\parallel}$ . Clean conductance quantization is measured [15] and, with respect to  $B_{\parallel}$ , Zeeman splitting is clearly seen. We observe the progressive evolution of the 1D subbands from the spin degenerate steps in units of  $2e^2/h$  at  $B_{\parallel} = 0$  T (leftmost arrow), to the complete spin-resolved quantized steps in units of  $e^2/h$  at  $B_{\parallel} = B_R \approx 3.6$  T (middle arrow). Further increasing  $B$  causes the 1D nondegenerate subbands to cross, leading to conductance plateaus quantized in units of half-odd multiple values of  $2e^2/h$  at  $B_{\parallel} = B_C \approx 7.6$  T (rightmost arrow). In Fig. 1(b), we plot the transconductance  $dG/dV_{\text{SG}}$  as a function of side gate voltage and  $B$

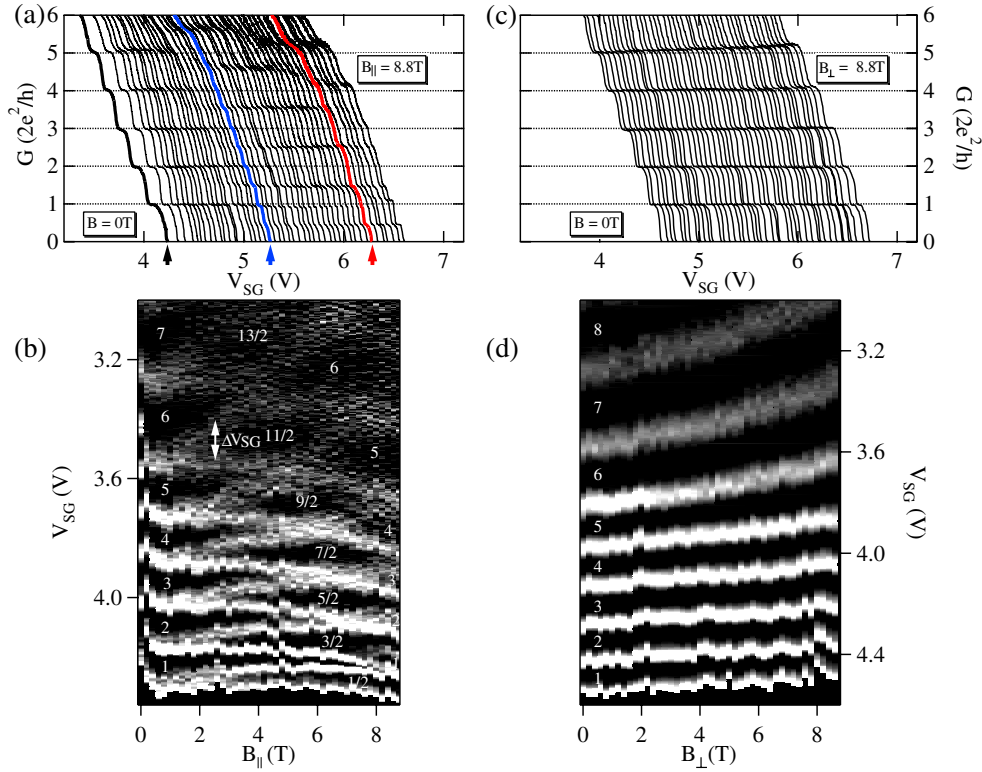


FIG. 1 (color online). (a) Differential conductance  $G$ , corrected for a series resistance, of the quantum wire for different in-plane magnetic fields parallel to the wire ( $B_{\parallel}$ ) from 0 to 8.8 T in steps of 0.2 T (from left to right).  $T = 20$  mK, back and middle gates are at 2.5 and  $-0.5$  V, respectively. All curves are shifted by 0.05 V for clarity. The second thicker curve (middle arrow) corresponds to  $B_{\parallel} = B_R$  when subbands are completely spin resolved; the third thicker curve (rightmost arrow) corresponds to  $B_{\parallel} = B_C$  when the subbands cross. (b) Corresponding transconductance gray scale as a function of  $V_{SG}$ ; black regions correspond to low transconductance (conductance plateaus, labeled with  $G$  in units of  $2e^2/h$ ); white regions correspond to high transconductance (subband edges). (c)  $G$  of the same quantum wire for different in-plane magnetic fields perpendicular to the wire ( $B_{\perp}$ ) under similar experimental conditions. (d) Corresponding transconductance gray scale as a function of  $V_{SG}$  and  $B_{\perp}$ .

(the derivative has been numerically calculated from  $G$  corrected for a series resistance). Crossings between non-degenerate 1D subband edges are clearly visible (white regions of the gray scale) as well as the diamond shape parts (in black) representing the conductance plateaus.

After thermal cycling and sample reorientation, we have measured the differential conductance for an in-plane magnetic fields perpendicular to the wire  $B_{\perp}$ . It is surprising to see in Figs. 1(c) and 1(d) that the well-quantized conductance steps are not affected by  $B_{\perp}$  up to 8.8 T. The transconductance gray scale shown in Fig. 1(d) highlights that no Zeeman splitting is seen when the magnetic field is aligned perpendicular to the wire.

In Fig. 2(a), we present a schematic view of the effect of an in-plane magnetic field on the spin degenerate 1D subbands. We assume that the splitting of a 1D energy subband is linear in magnetic field [16] and follows the equation  $\Delta E_N = g_N^* \mu_B B$ , where  $\Delta E_N$  is the Zeeman energy splitting of the  $N$ th degenerate subband,  $g_N^*$  is the effective Landé  $g$  factor of the  $N$ th degenerate subband,  $\mu_B$  is the Bohr magneton, and  $B$  is the applied magnetic field. In this diagram, the lines represent the subband edges as measured in Fig. 1(b). However, Zeeman splitting mea-

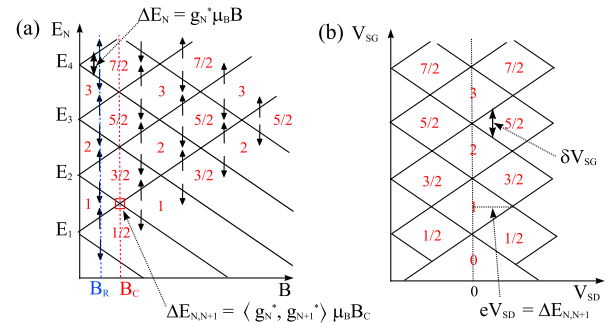


FIG. 2 (color online). (a) Schematic diagram of the Zeeman effect in a 1D system due to an in-plane magnetic field  $B$ : solid lines correspond to the 1D subband edges; spin orientations are given by the arrows. The first dotted line corresponds to  $B$  at fully resolved spin splitting  $B_R$ : at this stage, conductance steps are quantized in units of  $e^2/h$ . The second dotted line corresponds to 1D subband crossings at  $B_C$ : at this stage, conductance steps are quantized in half-odd multiples of  $2e^2/h$ . (b) Schematic of the transconductance for different  $V_{SD}$ : with this technique, it is possible to extract the spacing between two consecutive subbands (see [17–19]). Combined with Zeeman splitting measurement,  $g^*$  can then be found.

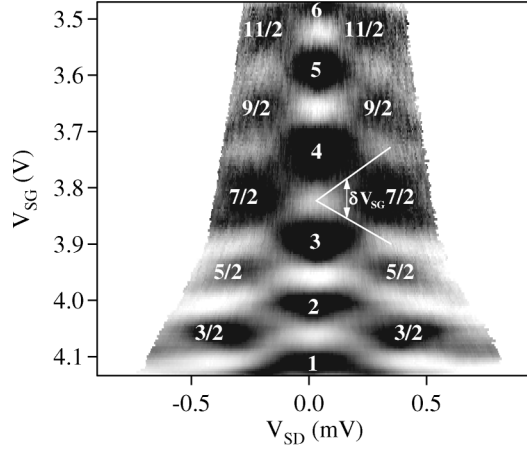


FIG. 3. Nonlinear transconductance gray scale at  $T = 20$  mK, back and middle gates are at 2.5 and  $-0.5$  V, respectively, and  $B = 0$  T as a function of  $V_{SD}$  [22]. The black parts correspond to low transconductance (plateaus). Quantized plateaus in units of  $2e^2/h$  at zero  $V_{SD}$  and extra plateaus for half-odd multiple values of  $2e^2/h$  at nonzero  $V_{SD}$  are labeled. Crossings of 1D subband edges are the white parts.

measurements, i.e., splitting of the transconductance peaks, is given in units of  $\Delta V_{SG}(B)$ . It is possible to convert  $\Delta V_{SG}(B)$  to  $\Delta E_N(B)$  and extract values of  $g^*$ , by combining Zeeman splitting measurements and source-drain bias  $V_{SD}$  spectroscopy [17]. In Fig. 2(b), we present a schematic of the transconductance as a function of the source-drain bias  $V_{SD}$  that allows the extraction of the subband spacings by tuning chemical potentials of the source and drain with respect to the 1D subbands ( $\Delta E_{N,N+1} = eV_{SD}$  at subband crossing), according to [17–19]. Figure 3 corresponds to a typical transconductance gray scale as a function of  $V_{SD}$ : clear half plateaus [17–19] (i.e., conductance plateau are quantized in units of half-odd multiple of  $2e^2/h$ ) are seen for high values of  $V_{SD}$  and 1D subband edges (in white) are visible.

A common way to extract  $g^*$  is to compare the crossing of two subband edges due to Zeeman splitting with that obtained from source-drain bias techniques [6] (if these crossings appear for the same  $V_{SG}$ ). We can relate bias voltage and energy:  $\Delta E_{N,N+1} = \langle g_N^*, g_{N+1}^* \rangle \mu_B B_C = eV_{SD}$ , where  $\langle g_N^*, g_{N+1}^* \rangle$  is the average value of the effective Landé  $g$  factor for degenerate subbands  $N$  and  $N + 1$  and  $B_C$  is the magnetic field at subband crossing [see Figs. 2(a) and 2(b) and  $\langle g_N^*, g_{N+1}^* \rangle$  values corresponding to solid circles in Fig. 4(b)]. Another way to relate gate voltage and energy is to combine the splittings of transconductance gray scale lines (i.e., transconductance peaks) from both source-drain bias and Zeeman effect [i.e., combine respectively  $\delta V_{SG}(V_{SD})$  and  $\Delta V_{SG}(B)$ ]. We can use the basic relation for the linear Zeeman splitting of a 1D subband  $\partial \Delta E_N / \partial B = (\partial \Delta E_N / \partial V_{SG})(\partial V_{SG} / \partial B) = g_N^* \mu_B$ . Indeed, Zeeman splitting of the transconductance lines (i.e., transconductance peaks) give the 1D degenerate subband splitting differential change with respect to  $B$ ,  $\Delta V_{SG}(B)$  [see

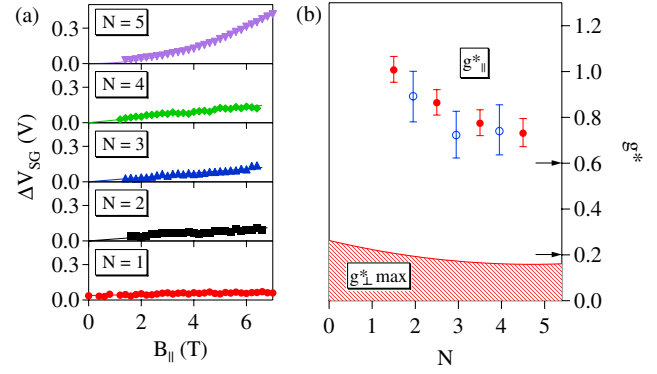


FIG. 4 (color online). (a)  $\Delta V_{SG}$  vs  $B_{\parallel}$  for the five first subbands; (b)  $g^*$  as a function of the subband index  $N$  extracted from the Zeeman splitting measurement and the  $V_{SD}$  spectroscopy: Solid circles are the average effective Landé  $g$  factor in the direction parallel to the wire, between two consecutive subbands  $\langle g_N^*, g_{N+1}^* \rangle$  given by subband-edge crossing measurements [6]. Open circles are extracted from the slope of the subband-edge splitting differential change technique for the  $B_{\parallel}$  pointing along the wire. The upper line of the striped part represents an upper bound of  $g^*$  for  $B_{\perp}$  perpendicular to the wire: this limit is determined by comparing the starting point of the 1D subband splittings ( $B_{\parallel} \approx 1.9$  T) and the maximum value of  $B_{\perp}$  ( $= 8.8$  T). The arrows define the absolute values of  $g^*$  calculated for a 20 nm quantum well of HH grown on (311)A surface [4,11]: the upper and lower arrows mark  $g^*$  for  $B$  pointing along  $[2\bar{3}3]$  and  $[01\bar{1}]$ , respectively.

Fig. 2(a)]. The slope of  $\Delta V_{SG}(B)$  corresponds to  $\partial V_{SG} / \partial B$ .  $V_{SD}$  spectroscopy provides the conversion factor between gate voltage and energy, given by the slope of  $\delta V_{SG}(V_{SD})$ ,  $\delta V_{SG} / eV_{SD}$ . Finally,  $g^*$  for the  $N$ th subband is  $g_N^* \mu_B = (eV_{SD} / \delta V_{SG})(\Delta V_{SG} / B)$  [ $g^*$  values extracted from this second technique correspond to the open circles in Fig. 4(b)].

In Fig. 4(a) we show the splitting of the transconductance peaks, i.e., the splitting of the 1D subband edges, represented by  $\Delta V_{SG}$  as a function of  $B$  for the first five 1D subbands. The spin splitting can be considered to be linear in  $B$  for the four first subbands. The fifth 1D subband clearly shows a deviation from a purely linear Zeeman splitting as the 1D system is becoming more 2D. Figure 4(b) displays  $g^*$  as a function of the degenerate 1D subbands index  $N$ : Remarkably, values and behavior of  $g_{\parallel}^*(N)$  for  $B_{\parallel}$  parallel to the wire are similar as found in previous results for electron quantum wires [6–8]. Because no sign of the beginning of spin splitting is detected for  $B$  applied perpendicular to the wire up to  $B_{\perp} = 8.8$  T, we can provide only maximum values of  $g_{\perp}^*$  in this orientation; the minimum  $g^*$  ratio  $g_{\parallel}^* / g_{\perp}^*$  can be estimated at least to be 4.5. This anisotropy is significantly stronger than in 2D HH systems [4,10,11]. Here, we provide an explanation with detailed calculations to be presented elsewhere [20].

In a quantum-confined structure, Zeeman splitting of HH states is suppressed unless the magnetic field is applied parallel to the natural quantization axis for total angular momentum  $\hat{J}$  [4]. This is a result of *strong spin-orbit*

*coupling in the valence band.* For a 2D system, this axis is perpendicular to the plane in which the holes are confined. As a result,  $g^*$  for the field direction perpendicular to the plane is typically at least an order of magnitude larger than that for magnetic fields applied in the plane. Also, the cubic crystal anisotropy gives rise to an anisotropy of  $g^*$  for orthogonal in-plane field directions [11]. In our 1D hole system, in addition to the large anisotropy of  $g^*$  for  $B_{\parallel}$  and  $B_{\perp}$ , we also measured a considerably larger value of  $g_{\parallel}^*$  for the lowest 1D subbands than was predicted theoretically [4] for the 20 nm wide quantum well as used in our sample. These findings can be explained by the fact that a 1D confinement tends to favor a quantization axis of  $\hat{J}$  parallel to the wire, i.e., perpendicular to the directions in which hole motion is quantized. Hence a large Zeeman splitting results when  $B$  is applied in the same direction. For  $B$  applied perpendicular to the wire, no direct Zeeman coupling between HH states exists, and their spin splitting arises only as a second-order effect from the HH-light holes (LH) couplings that are due to  $B$  and confinement. It is therefore suppressed by the confinement-induced energy splitting between the HH and LH 1D subbands. For our hole quantum wires, the confinement in the [311] direction given by the quantum well can still be expected to be stronger than the confinement in the lateral direction, i.e., [01 $\bar{1}$ ]. Nevertheless, the monotonic increase of  $g_{\parallel}^*$  over the 2D value of 0.6 [4,11], which is exhibited in Fig. 4, as the wire is made narrower (i.e., for smaller subband index  $N$ ) clearly indicates the expected trend. Note also that the direct HH Zeeman splitting for fields parallel to the wire could be enhanced by exchange effects, whereas the peculiar nature of spin-3/2 states usually prevents exchange enhancement of in-plane HH spin splittings in the 2D case [21]. However, both the Zeeman splitting and its exchange enhancement remain suppressed for directions perpendicular to the wire, due to the same reasons causing this suppression for in-plane field directions in a 2D HH system. This is in clear contrast to the electron systems where exchange enhancement of Zeeman splitting is isotropic [7].

In conclusion, we have studied the Zeeman splitting of hole quantum wires in the ballistic regime. We uncovered a very strong anisotropy of the effective Landé  $g$  factor for  $B$  parallel and perpendicular to the quantum wire. The 1D confinement significantly increases the anisotropy existing in the 2D HH system, known as a consequence of the SO coupling. This result opens a new way to engineer spin splitting in 1D nanostructures.

R.D. thanks S.E. Andresen, N. Kemp, and D. MacGrouther for useful comments on the manuscript. U.Z. thanks O.P. Sushkov for enlightening discussions. U.Z. is partially supported by the Marsden Fund of the Royal Society of New Zealand and acknowledges additional support from UNSW. M.Y.S. acknowledges additional support from the Australian Research Council Federation. This work has been funded by the Australian Research Council and the EPSRC.

\*Corresponding author.

Electronic address: r.danneau@unsw.edu.au

- [1] I. Žutić, J. Fabian, and S. Das Sarma, *Rev. Mod. Phys.* **76**, 323 (2004).
- [2] Yu.A. Bychkov and E.I. Rashba, *J. Phys. C* **17**, 6039 (1984).
- [3] S. Datta and B. Das, *Appl. Phys. Lett.* **56**, 665 (1990).
- [4] R. Winkler, *Spin-Orbit Coupling Effects in Two-Dimensional Electron and Hole Systems* (Springer, Berlin, 2003).
- [5] H.W. van Kesteren, E.C. Cosman, W.A.J.A. van der Poel, and C.T. Foxon, *Phys. Rev. B* **41**, 5283 (1990).
- [6] N.K. Patel *et al.*, *Phys. Rev. B* **44**, R10973 (1991).
- [7] K.J. Thomas *et al.*, *Phys. Rev. Lett.* **77**, 135 (1996).
- [8] K.J. Thomas *et al.*, *Phys. Rev. B* **58**, 4846 (1998).
- [9] A.J. Daneshvar *et al.*, *Phys. Rev. B* **55**, R13409 (1997).
- [10] S.J. Papadakis, E.P. De Poortere, M. Shayegan, and R. Winkler, *Phys. Rev. Lett.* **84**, 5592 (2000).
- [11] R. Winkler, S.J. Papadakis, E.P. De Poortere, and M. Shayegan, *Phys. Rev. Lett.* **85**, 4574 (2000).
- [12] In 2D HH systems, measurements of  $g^*$  are not possible due to the complexity of the hole band structure (see Ref. [4], p. 145 for a more complete explanation): The anisotropic Zeeman effect between  $[233]$  and  $[01\bar{1}]$  is observed by measuring the magnetic field  $B^*$  when the 2D HH is fully spin polarized. Experimental results in these systems found  $B_{[233]}^*/B_{[01\bar{1}]}^* \approx 1/2$  and theory predicted  $g_{[233]}^*/g_{[01\bar{1}]}^* \approx 4$  [4,10,11] (for a 20 nm quantum well). This anisotropy is independent of the current direction.
- [13] R. Danneau *et al.*, *Appl. Phys. Lett.* **88**, 012107 (2006).
- [14] The 2D HH system is confined in a 20 nm quantum well and has density  $1.2 \times 10^{15} \text{ m}^{-2}$  and mobility  $92 \text{ m}^2 \text{ V}^{-1} \text{ s}^{-1}$ .
- [15] Note that the conductance anomaly at  $0.7 \times 2e^2/h$ , which was observed in similar devices [13], does not appear for back and middle gates voltage (2.5 and  $-0.5$  V, respectively) used in the present experiment. The presence of the conductance anomaly is dependent on these gates voltages which contribute to modify the shape of the confinement potential.
- [16] F.F. Fang and P.J. Stiles, *Phys. Rev.* **174**, 823 (1968).
- [17] N.K. Patel *et al.*, *Phys. Rev. B* **44**, 13549 (1991).
- [18] L.I. Glazman and A.V. Khaetskii, *Europhys. Lett.* **9**, 263 (1989).
- [19] L. Martin-Moreno, J.T. Nicholls, N.K. Patel, and M. Pepper, *J. Phys. Condens. Matter* **4**, 1323 (1992).
- [20] U. Zülicke and O.P. Sushkov (to be published).
- [21] R. Winkler *et al.*, *Phys. Rev. B* **72**, 195321 (2005).
- [22] These data are taken from another cooldown than shown in Fig. 1.  $g^*$  is extracted from Zeeman splitting and  $V_{SD}$  spectroscopy taken from the same cooldown. To verify that the confining potential remains constant from one cooldown to the next, we measured the 1D subband spacings each time the device was thermally cycled. These were constant to within our experimental accuracy  $\pm 5\%$ .